

Lake Priyadarshini in the vicinity of the permanent Indian station, 'Maitri'. The map is a major advance over earlier maps prepared on the basis of manual survey. Earlier palaeoclimatic studies on lake sediments by Bera⁷, based on pollen analysis in a core collected from lake Priyadarshini, showed climatic changes over the past ~8000 yrs BP. In a recent study of the subsurface sediments collected from another lake (lat. 68°37'25.40"S and long. 77°58'15.20"E) in the Vestfold Hills region of Antarctica have been examined for foraminiferal content (both agglutinated and calcareous types of foraminiferal tests) along with arcellaceans, diatoms and ostracods (Figure 2) to assess the potential presence and application of foraminiferal proxies for reconstructing the geologic history of marginal Antarctic lakes.

The presence of foraminifera indicates marine influence in a few lakes. Additional efforts are underway to document temporal changes in the sediment grain size, pigments, diatoms, magnetic susceptibility of the sediments, etc. Once available, such multi-proxy data will be used to infer the past climatic and sea-level history. Deployment of improvised sediment traps is also envisaged for round-the-year monitoring of the bio-

logical and physico-chemical characteristics of the lakes.

GLIALPI is largely funded by the Ministry of Earth Sciences, Government of India, and undertaken to utilize the lake sediments to infer the Antarctic climatic history. However, unavailability of specialized coring device that can be operated under the extremely harsh conditions in Antarctica, has hampered the collection of long cores. Therefore global efforts similar to the Ocean Drilling Program and Deep-Sea Drilling Project, and continuation of programmes like ANDRILL and SHALDRILL are required to be implemented to collect long cores from different lakes in Antarctica, in order to generate regional climatic and sea-level change history. True to the spirit of the Antarctic treaty, GLIALPI is expected to emerge as a multi-institutional and multi-disciplinary collaborative programme and will support international programmes like ANDRILL and SHALDRILL.

1. Stone, R., *Science*, 1997, **278**, 1007.
2. EPICA community members, *Nature*, 2004, **429**, 623–628.
3. Alley, R. B., *Proc. Natl. Acad. Sci.*, 2000, **97**, 1331–1334.
4. Hodgson, D. A. *et al.*, *Quat. Res.*, 2005, **64**, 83–99.

5. Cromer, L., Gibson, G. A. E., Fwadling, K. M. and Hodgson, D. A., *J. Biogeogr.*, 2006, **33**, 1314–1323.
6. Backman, E. and Domack, E., Fall Meeting Abstract, American Geophysical Union, 2003, p. 31B-0256.
7. Bera, S., *Curr. Sci.*, 2004, **86**, 1485–1488.

Received 8 October 2007; revised accepted 6 November 2008

N. KHARE^{1,*}
R. SARASWAT²
R. RAVINDRA³

¹Ministry of Earth Sciences,
Mahasagar Bhawan,
Block # 12, CGO Complex,
Lodhi Road,
New Delhi 110 003, India

²Centre for Advanced Studies in Geology,
Department of Geology,
University of Delhi,
Delhi 110 007, India

³National Centre for Antarctic and
Ocean Research,
Headland Sada, Vasco-da-Gama,
Goa 403 804, India

*For correspondence.
e-mail: nkhare45@gmail.com

Coda Q_c attenuation in Indo-Myanmar region, Manipur, Northeast India

The elastic structure of the lithosphere is found to be inhomogeneous from various kinds of recent geological and seismological observations. The appearance of S -coda wave following direct S -phase in seismograms is an apparent evidence for the existence of such an inhomogeneity. The scattering and attenuation of high-frequency seismic waves are important to physically characterize the earth medium.

Seismic attenuation is usually considered to be a combination of two mechanisms, scattering loss and intrinsic absorption. Scattering redistributes wave energy within the medium. Conversely, intrinsic absorption refers to the conversion of vibration energy into heat. Wu¹ introduced the concept of seismic albedo B_0 as the ratio of scattering loss to total attenuation. There are several papers^{2–5}

which discuss mechanisms for intrinsic absorption that lead to frequency-independent Q_p^{-1} and Q_s^{-1} . Scattering loss to heterogeneities distributed in the earth causes a decrease in amplitude with travel distance⁶.

Recorded waveforms show a large variation in amplitude near the direct S arrival; the variation decreases as lapse time increases. S -coda waves have a common envelope shape at most stations near the epicentre after about twice the S -wave travel time⁷. The decay of these waves with time, in a seismogram, provides the average attenuation characteristics of the medium instead of the property of a single path connecting from a source to the station. The properties of the coda can be analysed by applying a statistical method requiring a small

number of parameters. Aki⁸, and Aki and Chouet⁹, pioneers in this field, proposed the backscattering model to use the coda waves of local earthquakes for estimation of quality factors (Q_c) in a region.

Q_c estimated using single backscattering model is strongly frequency-dependent. Frequency-dependent Q_c estimated for local earthquakes recorded at two broadband seismological observatories in Manipur valley is reported here. This has shed light on the attenuation characteristics of the subducted lithosphere at shallower depth (<70 km).

The digital data from seven earthquakes recorded by two stations equipped with digital broadband (BB) systems were analysed for the estimation of Q_c . The digital seismograms were recorded by the Guralp CMG40T Broadband Seismo-

meter at a sampling rate of 100 samples/s. Locations of the BB stations and epicentres of the events used for the analysis are shown in Figure 1, and details are given in Table 1.

A sample seismogram of *P*-wave, *S*-wave and coda waves recorded at the Ukhrul (UKH) observatory is illustrated in Figure 2. The backscattering model implies that scattering is a weak process and outgoing waves are scattered only once before reaching the receiver. Under this assumption the coda amplitudes $A(f, t)$ in a seismogram can be expressed for a central frequency f over a narrow bandwidth as a function of lapse time t , measured from the origin time of the seismic event, as¹⁰

$$A(f, t) = S(f)t^{-a} \exp(-\pi f t/Q_c),$$

where $S(f)$ represents the source function at frequency f and is considered a constant as it is independent of time and radiation pattern, and therefore not a function of factors influencing energy loss in the medium; a is the geometrical spreading factor and is taken as 1 for body waves, and Q_c is the apparent quality factor of coda waves representing attenuation in a medium. The above equation can be rewritten as

$$\ln[A(f, t)t] = C - bt,$$

where $b = \pi f/Q_c$ and $C = \ln S(f)$.

The above equation represents a straight line, the slope of which [$b(=\pi f/Q_c)$] provides the Q_c value at a central frequency, f . This equation has been used for estimation of Q_c for the earth crust below Manipur and adjoining areas in the Indo-Myanmar Region (IMR).

Each seismogram is filtered using Butterworth bandpass filter of eight poles. Nine frequency bands (bandwidth $0.67f_c$, where f_c is the central frequency) are used for this purpose. Low cut-off frequencies of these bands are given in Table 2. Seismograms thus filtered are used for a detailed study of the decay of coda wave amplitudes with time, to estimate Q_c at nine central frequencies. Coda waves of a fixed time window of 30 s for each filtered seismogram, which start from the lapse time $t = 2t_s$, where t_s is the direct *S*-wave travel time⁷ are chosen for the analysis. The 30 s coda windows of all the filtered seismograms from lapse time t onwards are smoothed using a root mean square (rms) technique.

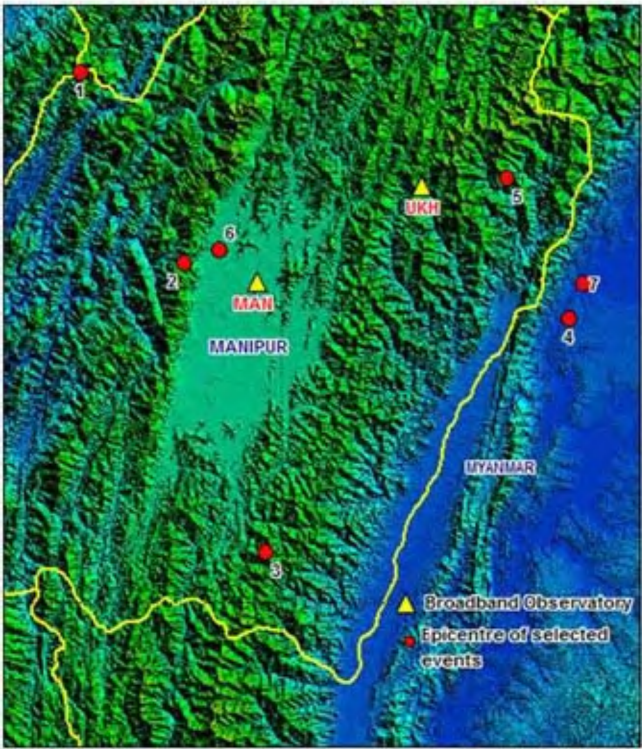


Figure 1. Observatories and epicentral locations of events used for coda quality factor (Q_c) analysis. Numbers indicate the serial numbers of events in Table 1.

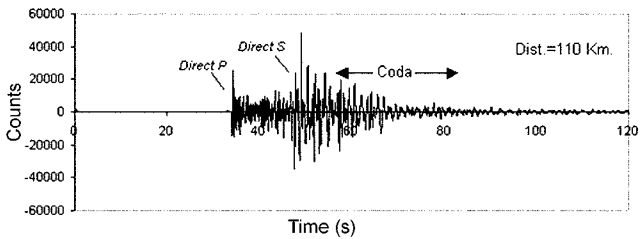


Figure 2. Example of original waveforms of an earthquake recorded on 20 February 2001 at UKH observatory.

Table 1. Selected events used in coda quality factor (Q_c) analysis

Sl. no.	Date	Origin time			Location		M_L	Focal depth (km)
		Hour	Minute	Second	Latitude (°N)	Longitude (°E)		
1	990405	22	32	59.13	25.25	93.48	4.1	65
2	990414	06	09	40.57	24.80	93.75	3.9	39
3	990415	20	18	11.26	24.12	93.96	4.1	60
4	000813	14	59	34.42	24.67	94.74	4.3	65
5	001104	10	04	45.19	25.00	94.58	3.8	40
6	010105	13	04	07.96	24.83	93.84	3.2	20
7	010426	21	01	31.64	24.75	94.78	4.8	23

Novelo *et al.*¹¹ compared different techniques that utilize the single scattering model using a time window of 5.12 and 2.56 s for 1.5 Hz and the remaining

higher frequencies respectively. This method has been adopted by many workers^{12,13} in scattering models. In the present study, we have calculated the rms

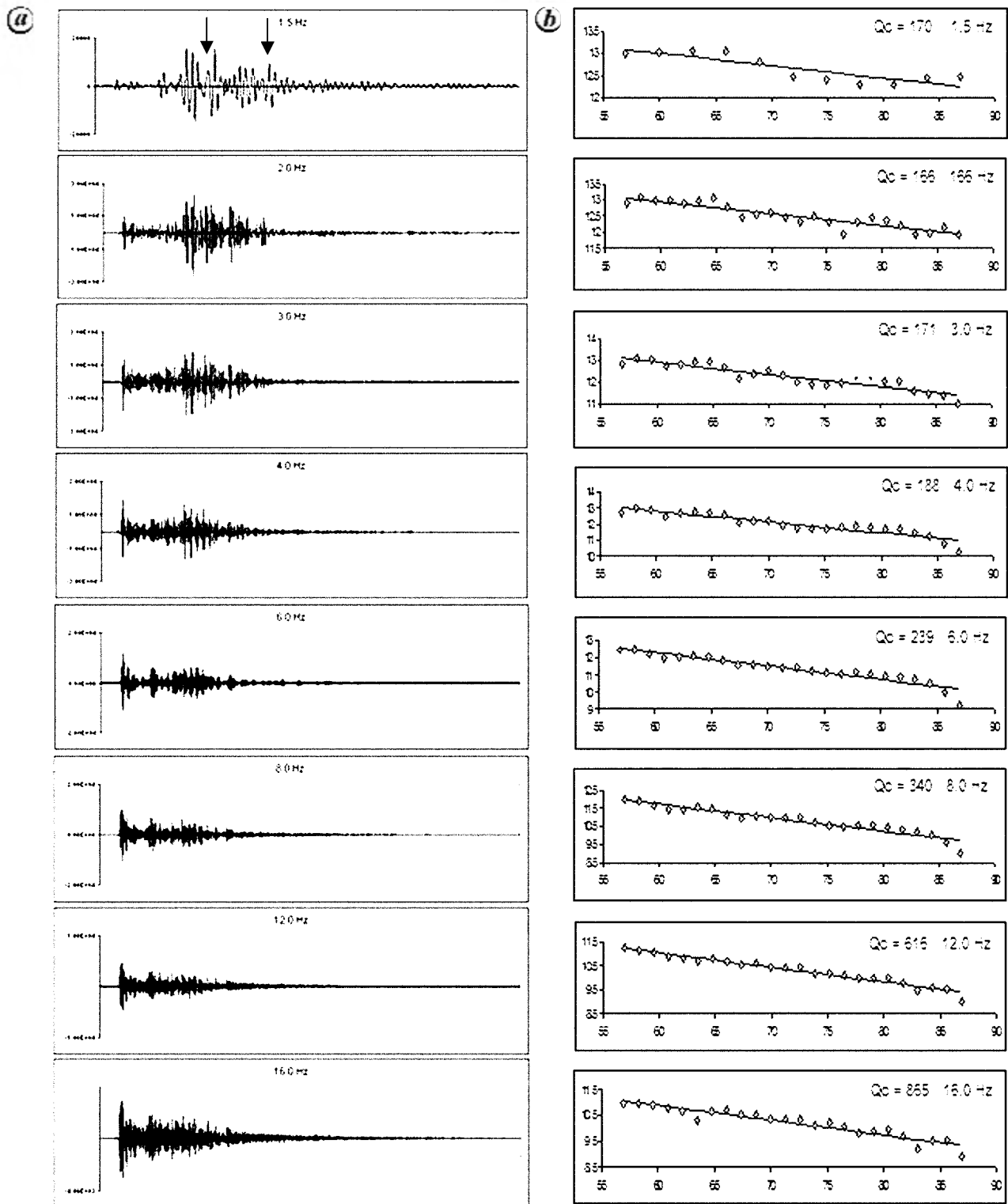


Figure 3. *a*, Example of original seismogram (Figure 2) and bandpass filtered coda waveforms. *b*, Corrected and smoothed logarithmic coda amplitude using the rms approach for the portion shown by arrows in (*a*). The straight lines are fitted in the least-squares sense. The estimated Q_c value for each frequency component is shown.

values of coda amplitude of the filtered seismograms in a time window of 5.12 s (for 1.5 Hz) and 2.56 s (for the remaining

central frequencies) with a sliding window along the coda in steps of half of the time window. The value at each step has

been evaluated in the same frequency band. The values obtained using this approach constitute a smoother envelope of

the coda. Figure 3 represents an example of the smoothed logarithmic amplitude of the coda part of the seismogram, in which the effect of geometrical spreading has been corrected for all the filtered seismograms. The respective values of Q_c are also given with each plot.

The Northeast Indian region is tectonically complex, with collision tectonics in the northeast Himalaya and subduction tectonics in the IMR. The IMR region is seismically more active in the Northeast Indian region due to northeastward un-

derthrusting of the Indian plate beneath the Burmese arc in eastern Manipur. The earthquakes show a dipping seismic zone below the IMR¹⁴, and depth of the subducted lithosphere goes down to 200 km. Hypocentres of the selected earthquakes in this study, however, fall at a depth range of 20–65 km (Table 1) in the upper part of the subducting lithosphere. Magnitude M_w of these earthquakes is 3.5–4.5. Q_c has been estimated using single backscattered model. Eight frequency bands of central frequency, 1.5, 2.0, 3.0,

4.0, 6.0, 8.0, 12.0, 16.0, have been used for this purpose.

From the analysis of coda waves of 30 s window length, a total 56 Q_c measurements were made in the eight frequency bands. Values of Q_c vary from 82 to 283 at frequency 1.5 Hz, and 865 to 3203 at frequency 16 Hz. Variation of Q_c as a function of frequency is plotted in Figure 4. The variation of Q_c at different central frequencies may be attributed to different factors: (i) difference in local site geological conditions of recording stations, (ii) difference in focal depth and (iii) difference in epicentral distance. To provide an average Q_c of the region, the mean value of Q_c was estimated from all the observed values at each central frequency (Figure 4). The plot of Q_c values as a function of frequency shows a definite dependence on frequency. By fitting the mean values of Q_c (given in Table 3), to the power law $Q_c = Q_0 f^n$, the frequency-dependent average Q_c relationship is obtained for the region as $Q_c = (109 \pm 28)f^{(0.964 \pm 0.12)}$. Estimating the Q_c values by changing the lapse time to 50 s, we obtain $Q_c = (123 \pm 31)f^{(1.11 \pm 0.2)}$. A significant dependence of Q_0 has been verified with the same datasets. Q_0 increases from 109 ± 28 to 123 ± 31 by increasing the lapse time (30–50 s). However, the same is not true for the exponent n , as it changes from 0.964 ± 0.12 to 1.11 ± 0.2 only. This is due to the fact that there is lapse-time dependence of Q_c , while n is not lapse-time dependent.

Several researchers have reported that seismically active regions display a low value of Q_0 , defined as Q_c at 1 Hz, which represents the level of medium heterogeneities, while stable shield-type structure shows high values^{15–17}. The level of tectonic activity in a region, on the other hand, can be correlated with the degree of frequency dependence n . Higher n value (~ 1) has been observed for tectoni-

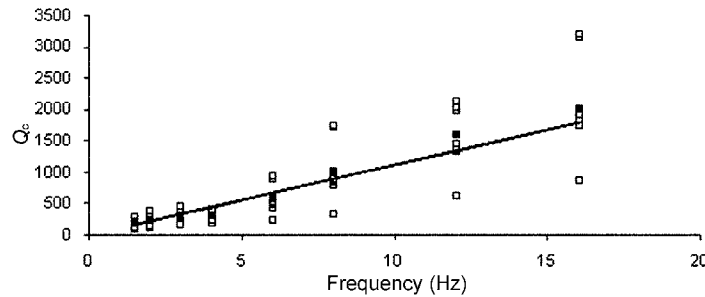


Figure 4. Q_c values at different frequencies for different events, with the regression line fitted.

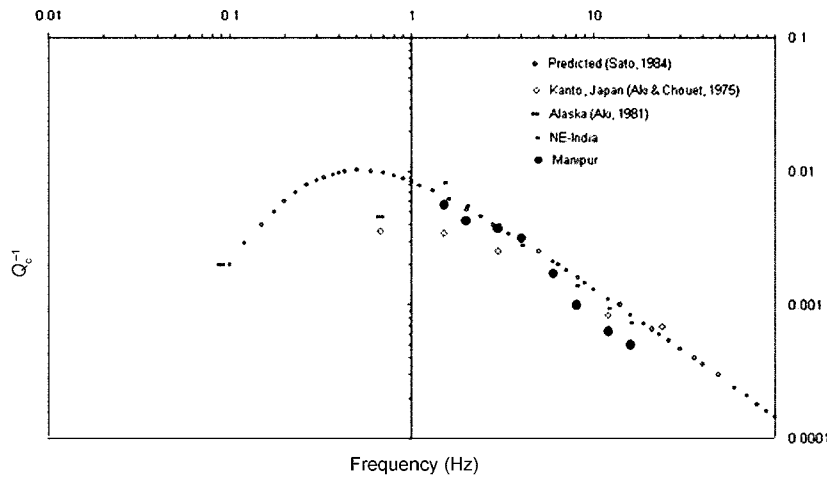


Figure 5. Comparison of frequency dependence of coda Q_c estimates in the present study with other reported values.

Table 2. Central frequency of bandpass filter with low and high cut-off frequencies

Low cut-off	Central frequency, f (Hz)	High cut-off
1.00	1.5	2.00
1.33	2.0	2.67
2.00	3.0	4.00
2.67	4.0	5.33
4.00	6.0	8.00
5.33	8.0	10.67
8.00	12.0	16.00
10.67	16.0	21.33

Table 3. Mean Q_c values at different frequencies

Frequency (Hz)	Q_c
1.5	179.2
2.0	232.9
3.0	264.13
4.0	312.90
6.0	578.88
8.0	1015.42
12.0	1596.54
16.0	2016.65

cally active regions compared to tectonically stable regions, where n is low. For central Asia, Roecker *et al.*¹⁶ reported that while Q_c increases with depth, the frequency dependence decreases from $\sim f^{1.0}$ at depth ~ 100 km to $\sim f^{0.75}$ at depth ~ 400 km. Pulli¹⁸ investigated lapse-time dependence of Q_c for New England from a dataset having depth from the surface to 500 km. He observed $n = 0.95$ for lapse time < 100 s, 0.95 for lapse time < 100 s and 0.40 for lapse time > 100 s. Results from both these regions provide information for a wider area with greater depth extent. For tectonically active regions and short coda window length^{17,19}, Q_c is often small (≈ 100) and n may be up to 1. Gupta and Kumar²¹ compared the Koyna and Garhwal Himalayan regions for the time-lapse window from 20 to 50 s; where n ranges from 1.02 to 1.09. These observations indicate that both the regions are tectonically active. They further reported $n = 1.02$ for Northeast India. In the present study, the estimate of n in Manipur for a 30 s window with a time lapse twice the S -travel time was 0.964, which is comparable with earlier observations²⁰.

The coda Q_c values in the present study have been compared with other subduction regions (Figure 5). In the Indo-Myanmar subduction zones, the shallower part of the lithosphere is characterized by $n = 0.964$ in this study, which can be correlated with other sub-

duction zones in the world (Figure 5). It has been observed that the upper part of the subducted lithosphere beneath the Manipur valley is tectonically active where $Q_c = (109 \pm 28)f^{(0.964 \pm 0.12)}$. The low Q_c values in the IMR reflect the strong scattering effects of highly dense faulted structures. Seismic activity is, however, more intense from the intermediate to deeper parts (70–200 km) of the lithosphere; this deeper zone needs to be understood in terms of Q_c in a future study. Since the present study is limited to only seven seismic events for estimating Q_c , more number of events (> 50) are to be used for coda analysis in the future studies to achieve the refined results in this seismically active region.

1. Wu, R. S., *Geophys. J. R. Astron. Soc.*, 1985, **82**, 57–80.
2. Knopoff, L., *Q. Rev. Geophys.*, 1964, **2**, 625–660.
3. Jackson, D. D. and Anderson, D. L., *Rev. Geophys. Space Phys.*, 1970, **8**, 1–63.
4. Marko, G. M. and Nur, A., *Geophysics*, 1979, **44**, 161–178.
5. Dziewonski, A. M., *Rev. Geophys. Space Phys.*, 1979, **17**, 303–312.
6. Aki, K., *Phys. Earth Planet. Inter.*, 1980, **21**, 50–60.
7. Rautian, T. G. and Khalturin, V. L., *Bull. Seismol. Soc. Am.*, 1978, **68**, 923–948.
8. Aki, K., *J. Geophys. Res.*, 1969, **74**, 615–631.
9. Aki, K. and Chouet, B., *J. Geophys. Res.*, 1975, **80**, 3322–3342.

10. Sato, H. and Fehler, M., *Seismic Wave Propagation and Scattering in the Heterogeneous Earth*, AIP Press/Springer-Verlag, New York, pp. 1–308.
11. Novelo-Casanova, D. A. and Lee, W. H. K., *Pure Appl. Geophys.*, 1991, **135**, 77–89.
12. Cherry, R. H., *Rev. Sci. Instrum.*, 1996, **67**, 215.
13. Şakir, Ş., *J. Seismol.*, 2008, **12**, 367–376.
14. Kayal, J. R., *Himalayan Geol.*, 1996, **17**, 53–69.
15. Herrmann, R. B., *Bull. Seismol. Soc. Am.*, 1980, **70**, 447–468.
16. Roecker, S. W., Tucker, B., King, J. and Hatzfeld, D., *Bull. Seismol. Soc. Am.*, 1982, **72**, 129–149.
17. Singh, S. and Herrmann, R. B., *J. Geophys. Res.*, 1983, **88**, 527–538.
18. Pulli, J. J., *Bull. Seismol. Soc. Am.*, 1984, **74**, 1149–1166.
19. Herraiz, M. and Espinosa, A. F., *Pure Appl. Geophys.*, 1987, **125**, 499–577.
20. Gupta, S. C. and Ashwani Kumar, *Curr. Sci.*, 2002, **82**, 407–413.

Received 18 October 2007; revised accepted 6 November 2008

S. MANICHANDRA
ARUN KUMAR*

Department of Earth Sciences,
Manipur University,
Imphal 795 003, India

*For correspondence.

e-mail: arun_kumar610@yahoo.com